Feedback Control Strategy to Eliminate the Input Current Harmonics of Matrix Converter Under Unbalanced Input Voltages

Jiaxing Lei, *Student Member, IEEE*, Bo Zhou, Jinliang Bian, Jiadan Wei, *Member, IEEE*, Yiqi Zhu, Jiang Yu, and Yang Yang

***Abstract*—It is generally considered that feedback control of input currents in the matrix converter (MC) is hard to be realized due to the coupling of input control and output control, which reduces the degree of freedom and robustness. Moreover, under unbalanced input voltages, the coupling also results in severe distortion of input currents when the commonly used feedforward compensation control method with fixed input power factor is adopted. To address these two issues, this paper proposes a feedback control strategy on the input side of MC. This strategy is based on a control method which can modify input reference currents. The input control strategy is embedded into the output control strategy and thus is the inner loop of the system control. The input-side controllers can be designed to achieve expected input control objectives and maintain the output performance at the same time. On this basis, resonant controllers are applied to regulate input currents and instantaneous active power, so as to directly eliminate the input current harmonics and meanwhile ensure the load absorbing constant active power under unbalanced input voltages. The validity and feasibility of the proposed strategy are verified by the simulation and experimental results.**

***Index Terms*—Feedback control, input current control, matrix converter, resonant controller, sinusoidal input currents, unbalanced input voltages.**

I. Introduction

MATRIX converter (MC) is a direct ac–ac power converter, featuring no energy storage elements on the dc bus. Compared with back-to-back (B2B) voltage-source converter, MC has the advantages of smaller volume and lighter weight [1], [2], and has been applied to motor drives [3], unified power flow controller [4], distributed generation system [5], etc.

Due to the lack of energy storage elements on the dc bus, the input control and output control of MC are closely coupled [6]. A general opinion in literature is that the coupling leads to a lower degree of freedom and less robustness of MC than the B2B converter [1], [6]. This is because the phase angle of input current vector can be predetermined, but the amplitude has to adjust itself passively through the load current segments [1], [6]. Therefore, the input current control is not directly controlled and MC does not allow for feedback control of input currents. Haruna and Itoh [7] tried to apply closed-loop control based on PID controllers to the regulation of input currents. However, the authors of [7] then found that the feedback control on the input side turned out to be conflicted with that on the output side [8], which could degrade output performance and thus was of low practical value.

On the other hand, the input–output coupling enables the input disturbances to be transferred directly to the load, thereby influencing the waveform quality on the output side. In practical application, the utility grid usually serves as the power supply of MC and thus input voltages are likely to be unbalanced due to the numerous asymmetric loads in the power grid. To avoid low-order harmonics in output currents resulting from input unbalance, the input control and output control need to coordinate with each other [9]. The most common control method in practice is the feedforward compensation of input voltage amplitude [10]. In this method, the real-time values of three-phase input voltages are measured to calculate their instantaneous amplitude. Then, the modulation index of MC is corrected according to the obtained input voltage amplitude. Besides, the input power factor angle is usually fixed at a constant value (e.g., 0 to achieve unit power factor operation). Casadei *et al.* [11] proved that this common method would result in considerable third, fifth, and other odd order harmonics in input currents when the input voltages were unbalanced. Consequently, the highly distorted input currents lead to poor quality of power supply. Therefore, it is necessary to reduce input current harmonics of MC under unbalanced input voltages. Casadei *et al.* [11] proposed an improved control method which dynamically modified the input power factor angle according to the positive and negative sequence components of input voltages, rather than fixing it at a constant value. Simulation and experimental results [11]–[13] demonstrated that this improved control method could obtain sinusoidal input currents when input voltages are unbalanced, while does not influence the waveform quality of output currents. The idea of this method is adopted by some researchers. Similar control methods for sinusoidal input currents were realized in [14] and [15] based on enhanced double-line voltage

Manuscript received September 11, 2015; revised January 12, 2016; accepted February 29, 2016. Date of publication March 8, 2016; date of current version September 16, 2016. This work was supported in part by the National Natural Science Foundation of China under Grant 51177069, by the Fundamental Research Funds for the Central Universities under Grant NP2015205, and by the Jiangsu Innovation Program for Graduate Education under Grant KYLX_0269. Recommended for publication by Associate Editor J.-i. Itoh.

J. Lei, B. Zhou, J. Bian, J. Wei, and Y. Zhu are with the Jiangsu Key Laboratory of New Energy Generation and Power Conversion, College of Automation Engineering, Nanjing University of Aeronautics and Astronautics, Nanjing 210016, China (e-mail: ljxnuaa@nuaa.edu.cn; zhoubo@nuaa.edu.cn; bjlnuaa@nuaa.edu.cn; weijiadan@nuaa.edu.cn; echo_yiqi@nuaa.edu.cn).

J. Yu and Y. Yang are with Shaanxi Aero Electric Co., Ltd., Aviation Key Laboratory of Science and Technology on Aerospace Power System, Xingping 713107, China (e-mail: jiang115yu@163.com; masayoung@163.com).

Color versions of one or more of the figures in this paper are available online at http://ieeexplore.ieee.org.

Digital Object Identifier 10.1109/TPEL.2016.2539398

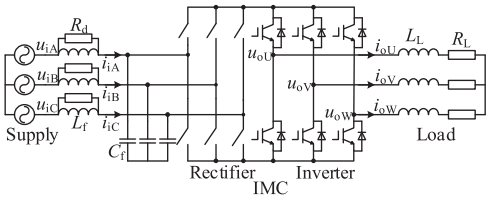

Fig. 1. Structure of the MC system.

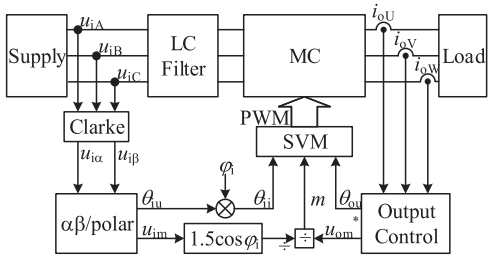

Fig. 2. Conventional control method of feedforward compensation with fixed input power factor angle [10].

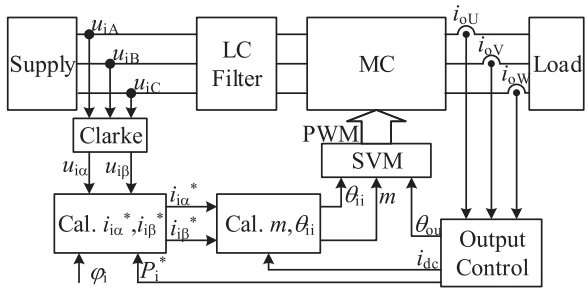

Fig. 3. Improved control method of MC in [20].

synthesis algorithm, in [16] with online optimization of duty cycles, and in [17] utilizing mathematical construction method. In addition, Li *et al.* [17] showed that if the input current vector angle was only imposed along the positive sequence vector of input voltages, the harmonics content of input currents was less than the conventional control method presented in [10] but larger than the improved method in [11]. Lei *et al.* [18] simplified the realization of the improved method in [11], which only needed a notch filter to obtain the expected input power factor angle. Yet, most of these methods were highly dependent on the sequence decomposition algorithms and/or input voltage sampling.

In voltage-source converters, it is common to eliminate input current harmonics under unbalanced input voltages by incorporating resonant controllers into the closed-loop control method of input currents [19]. However, there is no corresponding achievement for MC due to the general opinion that feedback control of input currents is difficult to realize. Lei *et al.* [20] presented a control method for MC which could directly control input currents without affecting the output performance. This control method enables the realization of a novel active damping control strategy of equivalent damping performance with passive damping control. Based on the method in [20], a feedback control strategy on the input side of MC is proposed in this paper. This strategy includes closed-loop control of input currents and input active power. In this control strategy, resonant controllers are adopted to regulate input currents and active power, so as to eliminate the input current harmonics directly and keep the active power constant as required by load. Compared with the conventional control method, the proposed method can improve the waveform quality of input currents dramatically without degrading the waveform quality of output currents.

This paper is organized as follows: Section II presents the proposed feedback control strategy on the input side of MC; Section III discusses the harmonic distribution of input currents under unbalanced input voltages and the controller design to eliminate the current harmonics; Section IV introduces the simulation and experimental results; Section V draws the conclusion.

II. Feedback Control Strategy on the Input Side of MC

A. Conventional Control Method

Fig. 1 illustrates the MC system structure studied in this paper. The indirect matrix converter (IMC), which is composed of a rectifier stage and an inverter stage, serves as the ac–ac power converter between power supply and load. IMC can also be replaced by direct matrix converter since they have the same function [1].

The principle of the conventional control method presented in [10] is shown in Fig. 2. The three-phase input voltages $u_{\rm iA}$, $u_{\rm iB}$, and $u_{\rm iC}$ are sampled to calculate their $\alpha\beta$-axis components $u_{i\alpha}$ and $u_{i\beta}$ via Clarke transformation. Based on polar transformation, the instantaneous amplitude $u_{\rm im}$ and phase angle $\theta_{\rm iu}$ of input voltage vector are obtained. The input power factor angle φ_i which is usually fixed at 0 for unit power factor operation is added into $\theta_{\rm iu}$, and then the phase angle $\theta_{\rm ii}$ of input current is obtained. $u^*_{\rm om}$ and $\theta_{\rm ou}$ are the amplitude and phase angle of the expected output voltage vector separately, which are generated by open-loop or closed-loop output control. The modulation index *m* is calculated with $u_{\rm im}$, $u^*_{\rm om}$, and φ_i. After *m*, $\theta_{\rm ii}$, and $\theta_{\rm ou}$ are obtained; the space vector modulation (SVM) algorithm can be implemented in digital controller [21].

B. Improved Control Method to Make Input Reference Currents Modifiable [20]

Fig. 1 shows that when the conventional control method generates the modulation signals *m*, $\theta_{\rm ii}$, and $\theta_{\rm ou}$, only the phase angle $\theta_{\rm ii}$ of input current vector is directly controlled, but not the amplitude. This is the reason why MC does not allow for the feedback control of input currents [1], [6], [22]. Lei *et al.* [20] present an improved control method, of which the principle is illustrated in Fig. 3. In this method, the output control produces the expected value P_i^* of active power and the dc-bus current $i_{\rm dc}$ defined in [20]

$$P_i^* = 1.5\left(u^*_{o\alpha}i_{o\alpha} + u^*_{o\beta}i_{o\beta}\right) \tag{1}$$

$$i_{\rm dc} = \frac{\sqrt{3}(u^*_{o\alpha}i_{o\alpha} + u^*_{o\beta}i_{o\beta})}{2u^*_{\rm om}} \tag{2}$$

where $u_{o\alpha}^*$ and $u_{o\beta}^*$ are the $\alpha\beta$-axis components of output reference voltages; $i_{o\alpha}$ and $i_{o\beta}$ are the $\alpha\beta$-axis components of output currents. P_i^* and $i_{\rm dc}$ can also be calculated in rotating frame. Based on instantaneous power theory [23], the input reference currents $i_{i\alpha}^*$ and $i_{i\beta}^*$ is obtained from (1)

$$\begin{cases} i_{i\alpha}^* = \dfrac{P_i^*\left(u_{i\alpha} - \tan\varphi_i u_{i\beta}\right)}{1.5(u_{i\alpha}^2 + u_{i\beta}^2)} \\ i_{i\beta}^* = \dfrac{P_i^*\left(u_{i\beta} + \tan\varphi_i u_{i\alpha}\right)}{1.5(u_{i\alpha}^2 + u_{i\beta}^2)}. \end{cases} \tag{3}$$

After $i_{i\alpha}^*$ and $i_{i\beta}^*$ are obtained, the modulation index m and the input current vector angle $\theta_{\rm ii}$ can be calculated [20]

$$\begin{cases} m = \sqrt{\left(\dfrac{i_{i\alpha}^*}{i_{\rm dc}}\right)^2 + \left(\dfrac{i_{i\beta}^*}{i_{\rm dc}}\right)^2} \\ \theta_{\rm ii} = a\tan 2\left(\dfrac{i_{i\beta}^*}{i_{\rm dc}}, \dfrac{i_{i\alpha}^*}{i_{\rm dc}}\right). \end{cases} \tag{4}$$

According to the analysis in [20], the improved control method shown in Fig. 3 has exactly the same input–output transfer function with the conventional control method shown in Fig. 2. However, the improved method could directly control the $\alpha\beta$-axis components (equivalently the amplitude and phase angle) of input currents. Therefore, it enables the realization of some input control strategies which require input currents to be directly controllable. For example, Lei *et al.* [20] modified the input reference currents with the derivations of actual values, realizing a novel active damping control strategy on the input side which has the same damping performance with passive damping control.

C. Block Diagram of the Proposed Control Strategy

Since the improved control method shown in Fig. 3 completely controls the input currents, a feedback control strategy on the input side of MC is developed by this paper, which is shown in Fig. 4. Fig. 4(a) shows the control block of the whole system while Fig. 4(b) illustrates the detailed structure of the input control strategy. As it can be seen from Fig. 4, the input control includes closed-loop control of input active power and input currents. $G_P(s)$ and $G_I(s)$ are the controllers on the forward path, respectively, while $F_P(s)$ and $F_I(s)$ are the controllers on the feedback path separately. The closed-loop control of input active power produces the modified reference values P_i^{**}, which are used to replace P_i^* in (3) to calculate the input reference currents $i_{i\alpha}^*$ and $i_{i\beta}^*$. The closed-loop control of input currents produces the modified input reference currents $i_{i\alpha}^{**}$ and $i_{i\beta}^{**}$, which are used to replace $i_{i\alpha}^*$ and $i_{i\beta}^*$ in (4) to calculate the modulation signals m and $\theta_{\rm ii}$. In Fig. 4, the actual input active and reactive power are calculated based on instantaneous power theory [23]

$$P_i = 1.5\left(u_{i\alpha}i_{i\alpha} + u_{i\beta}i_{i\beta}\right). \tag{5}$$

It is noted that the control strategy is given in stationary frame, so as to maintain the consistence of this paper, but it is certainly applicable to the rotating frame.

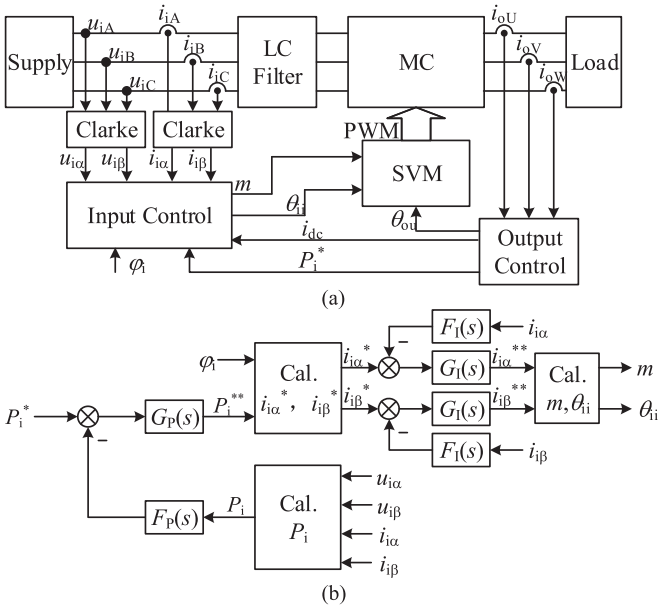

Fig. 4. Feedback control strategy on the input side of MC.

Fig. 4 shows that the feedback control on the input side is the inner loop of the whole system control, while the output control is the outer loop. Therefore, by designing appropriate controllers in the inner loop, it is possible to achieve some control objects on the input side without affecting the output performance. In Fig. 4(b), the closed-loop control of input currents is similar to that in voltage-source converters. However, the closed-loop control of input active power is specially designed for MC since its function is to maintain the active power constant as required by load, in case that the input current control influences the constant active power absorbed by load.

It should be stated here that the conventional control method shown in Fig. 1 can achieve satisfactory input performance under ideal conditions, and thus it is unnecessary to adopt the input feedback control strategy shown in Fig. 4. Nevertheless, in some cases, the input performance can be enhanced by the feedback control. For example, the feedback control strategy is applied to eliminate the input current harmonics under unbalanced input voltages, which will be introduced in Section III.

III. Elimination of Input Current Harmonics Under Unbalanced Input Voltages

In this section, the feedback control strategy shown in Fig. 4 is used to eliminate the input current harmonics caused by unbalanced input voltage. Section III-A introduces the harmonic distribution of input currents under unbalanced input voltages. Section III-B and C presents the controller design for the closed-loop control of input currents and active power, respectively. Section III-D proves that closed-loop control of input active power does not affect the performance of input current control. To simplify the control strategy, the input power factor angle φ_i is fixed at 0.

A. Input Current Harmonics With the Conventional Control Method

Supposing the input voltages are sinusoidal, the $\alpha\beta$-axis components can be expressed as [15]

$$\begin{cases} u_{i\alpha} = U_{\rm ip}\cos\left(\omega_i t + \varphi_{\rm iup}\right) + U_{\rm in}\cos\left(\omega_i t - \varphi_{\rm iun}\right) \\ u_{i\beta} = U_{\rm ip}\sin\left(\omega_i t + \varphi_{\rm iup}\right) - U_{\rm in}\sin\left(\omega_i t - \varphi_{\rm iun}\right) \end{cases} \tag{6}$$

where $U_{\rm ip}$ and $\varphi_{\rm iup}$ are the amplitude and phase angle of positive sequence voltage, while $U_{\rm in}$ and $\varphi_{\rm iun}$ are the amplitude and phase angle of negative sequence voltage; ω_i is the input voltage frequency. $U_{\rm in}$ is 0 if input voltages are balanced and is nonzero otherwise. By substituting (6) into (3) and analyzing the spectrum, the input reference currents can be expressed in the form of Fourier series [11]

$$\begin{cases} i_{i\alpha}^{*} = \dfrac{P_i^{*}\sum_{k=0}^{\infty}(-\lambda)^k\cos\left[(2k+1)\,\omega_i t + \varphi_{\rm iuk}\right]}{1.5\,U_{\rm ip}} \\ i_{i\beta}^{*} = \dfrac{P_i^{*}\sum_{k=0}^{\infty}(-\lambda)^k\sin\left[(2k+1)\,\omega_i t + \varphi_{\rm iuk}\right]}{1.5\,U_{\rm ip}} \end{cases} \tag{7}$$

where $\varphi_{\rm iuk}$ is phase angle of the $(2k+1)$th current harmonic; symbol λ is equal to $U_{\rm in}/U_{\rm ip}$, representing the unbalanced degree of input voltages.

According to Fig. 3, the conventional control method of feedforward compensation with fixed input power factor angle results in a lot of odd harmonics in the reference values of input currents, which are directly transferred into the actual values and thus lead to the degraded input power quality. In addition, as shown by (7), the ratio of the amplitude of $(2k+1)^{\rm th}$ harmonic component to that of the fundamental component is denoted as h_{2k+1}

$$h_{2k+1} = \lambda^k. \tag{8}$$

Therefore, h_{2k+1} is a power function of the unbalanced degree λ. Besides, h_{2k+1} drops exponentially with the harmonic order, since λ is generally less than 1.

In practice, the unbalanced degree λ of the grid voltages is usually less than 2% [24], but it could increase to more than 5% under abnormal condition. In this paper, the maximum of λ is supposed to be 15%, which could cover most practical cases. According to (8), when λ varies in the range of [0, 15%], the values of h_3, h_5, h_7, and h_9 which represent the contents of third, fifth, seventh and ninth harmonics are shown in Fig. 5. From Fig. 5, it is clear that the third harmonic is primary in the whole range. When λ increases, h_5 increases up to 2.25% which is also noticeable. On the contrary, h_7 and h_9 are less than 0.5% which are ignorable in the whole range. To sum up, the conventional control method results in many third and fifth input current harmonics which are necessary to be eliminated.

B. Controller Design for the Input Current Loop

According to the discussion in Section III-A, the input reference currents with conventional control method contain considerable third and fifth harmonics, which will directly be transferred into the actual currents. To eliminate the current harmonics, resonant controllers are applied to the closed-loop

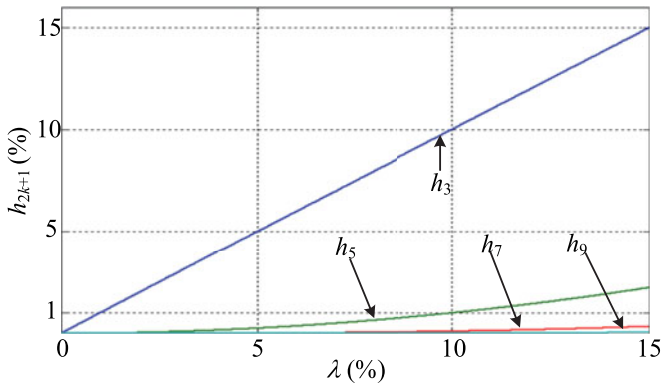

Fig. 5. Harmonic contents h_{2k+1} in input currents with the conventional control method, when the unbalanced degree λ varies in the range of [0, 15%].

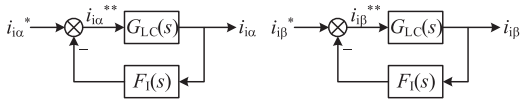

Fig. 6. Signal flow graphs of closed-loop control of $\alpha\beta$-axis input currents.

control of input currents. The designed controllers $G_I(s)$ and $F_I(s)$ are

$$G_I(s) = 1, \quad F_I(s) = \frac{K_{\rm RI3}s}{s^2 + (3\,\omega_i)^2} + \frac{K_{\rm RI5}s}{s^2 + (5\,\omega_i)^2}. \tag{9}$$

Namely, the forward path is directly feed through while the feedback controller $F_I(s)$ is composed of two resonant controllers in parallel, whose center frequencies are $3\,\omega_i$ and $5\,\omega_i$, respectively, and proportional coefficients are $K_{\rm RI3}$ and $K_{\rm RI5}$. Certainly, if the contents of seventh and ninth harmonics are also significant, resonant controllers whose center frequencies are seventh and ninth can be incorporated into $F_I(s)$ to eliminate these harmonics. However, as it can be seen from (8) and Fig. 5, the harmonic contents of seventh and above are less than 0.5% even when the unbalanced degree λ is up to 15%. Therefore, only the two controllers in (9) are adopted in this paper.

Ignoring the time-delay effect generated by pulse width modulation control of MC, the signal flow graphs of the closed-loop control of $\alpha\beta$-axis input currents are shown in Fig. 6. From Fig. 6, the closed-loop transfer function of input currents is

$$H_I(s) = \frac{G_{\rm LC}(s)}{1 + F_I(s)\,G_{\rm LC}(s)} \tag{10}$$

where $G_{\rm LC}(s)$ is the open-loop transfer function and is decided by the input *LC*-filter

$$G_{\rm LC}(s) = \frac{\frac{L_f}{R_d}s + 1}{L_f C_f s^2 + \frac{L_f}{R_d}s + 1}. \tag{11}$$

According to (9) and (11), the gains of $F_I(s)$ at the frequency of $3\,\omega_i$ and $5\,\omega_i$ are infinite [25] while the gains of $G_{\rm LC}(s)$ at these two frequencies are approximately unit. As a result, the gains of $H_I(s)$ at these two frequencies are zero, which can also be found from the frequency response of $H_I(s)$ shown

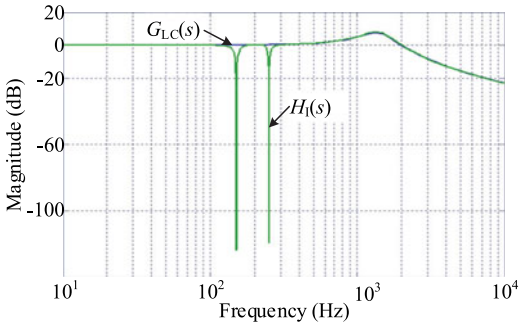

Fig. 7. Frequency responses of $G_{\mathrm{LC}}(s)$ and $H_I(s)$.

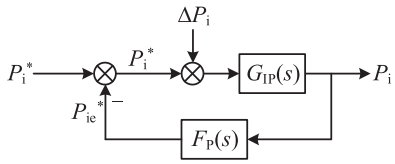

Fig. 8. Signal flow graph of closed-loop control of input active power.

in Fig. 7. To highlight the control performance of $H_I(s)$, the frequency response of $G_{\mathrm{LC}}(s)$ is also shown in Fig. 7. It can be seen from Fig. 7 that compared with $G_{\mathrm{LC}}(s)$, $H_I(s)$ reduces the gains at $3\,\omega_i$ and $5\,\omega_i$ to zero without changing the gains at the fundamental frequency and high frequencies. Therefore, the closed-loop control of input currents only eliminates the third and fifth harmonics, but does not affect the fundamental components and the filtering performance of the *LC* filter.

C. Controller Design for the Input Active Power Loop

According to the frequency response of $H_I(s)$, the closed-loop control of input currents can completely remove the third and fifth harmonics. Ignoring other minor harmonics, the actual input currents $i_{i\alpha}$ and $i_{i\beta}$ only contain fundamental components, which can be expressed as [11]

$$\begin{cases} i_{i\alpha} = \dfrac{P_i^* \cos\left(\omega_i t + \varphi_{\mathrm{iup}}\right)}{1.5\,U_{\mathrm{ip}}} \\ i_{i\beta} = \dfrac{P_i^* \sin\left(\omega_i t + \varphi_{\mathrm{iup}}\right)}{1.5\,U_{\mathrm{ip}}}. \end{cases} \tag{12}$$

By substituting (6) and (12) into (5) and performing some basic trigonometric function operation, the actual input active power P_i is obtained

$$P_i = P_i^* + \Delta P_i \tag{13}$$

where ΔP_i is the power disturbance and is expressed as follows:

$$\Delta P_i = \lambda P_i^* \cos\left(2\,\omega_i t + \varphi_{\mathrm{iup}} - \varphi_{\mathrm{iun}}\right). \tag{14}$$

Therefore, the actual input active power P_i is not equal to its reference value P_i^*, but is equal to P_i^* added with an ac component, whose frequency is $2\,\omega_i$ and amplitude is proportional to P_i^* and the unbalanced degree λ.

(13) shows that although the input current feedback control can eliminate the third and fifth current harmonics, it results in the harmonic of $2\,\omega_i$ in input active power. Due to the absence of dc-bus energy storage elements, this active power harmonic could directly be transferred to the output side, degrading the waveform quality of output currents.

To maintain the output performance, the resonant controller is further applied to the input active power feedback control. Similar to the input current feedback control, the resonant controller is also located in the feedback path, namely

$$G_P(s) = 1, \quad F_P(s) = \frac{K_{\mathrm{RP}}\, s}{s^2 + (2\,\omega_i)^2} \tag{15}$$

where K_{RP} is the proportional coefficient of $F_P(s)$.

According to Fig. 4(b) and (13), Fig. 8 shows the signal flow graph of closed-loop control of input active power. In Fig. 8, P_{ie}^* is the additional control signal generated by the feedback controller $F_P(s)$. $G_{\mathrm{IP}}(s)$ is the open-loop transfer function from P_i^* and ΔP_i to the active power P_i, which is decided by the input current control. In (13), $G_{\mathrm{IP}}(s)$ is ignored since only the steady-state value of active power is considered. However, in Fig. 8, $G_{\mathrm{IP}}(s)$ is added into the signal flow graph so as to analyze the closed-loop transfer function $H_P(s)$ of active power. From Fig. 8, the expression of $H_P(s)$ is

$$H_P(s) = \frac{G_{\mathrm{IP}}(s)}{1 + F_P(s)\, G_{\mathrm{IP}}(s)}. \tag{16}$$

TABLE I
AMPLITUDES OF THE THREE-PHASE INPUT VOLTAGES AND THE POSITIVE AND NEGATIVE SEQUENCE VOLTAGES UNDER DIFFERENT UNBALANCED DEGREES

λ (%)	U_{iA} (V)	U_{iB} (V)	U_{iC} (V)	U_{ip} (V)	U_{in} (V)
0	169.7	169.7	169.7	169.7	0.0
5	155.0		184.4		8.5
10	140.3		199.1		17.0
15	125.4		214.0		25.5

TABLE II
PARAMETERS OF THE EXPERIMENTAL PROTOTYPE

Variables	Description	Values
Input LC filter		
L_f	Filter inductor	1 mH
C_f	Filter capacitor	12.6 μF
R_d	Damping resistor	19 Ω
IMC power setup		
IGBT module	Power module of rectifier stage	APTGT50TDU60PG
	Power module of inverter stage	PM75RLA060
Load		
L_L	Load inductor	2 mH
R_L	Load resistor	7 Ω
F_o	Output frequency	80 Hz
Controller		
DSP	Digital signal processor	TMS320F28335
CPLD	Complex programmable logic device	EPM1270T144C8N
ADC	Analog-to-digital converter	ADS8568
DAC	Digital-to-analog converter	AD5438
f_{sampling}	Sampling frequency	20 kHz
$f_{\mathrm{switching}}$	Switching frequency of rectifier stage	10 kHz
	Switching frequency of inverter stage	20 kHz

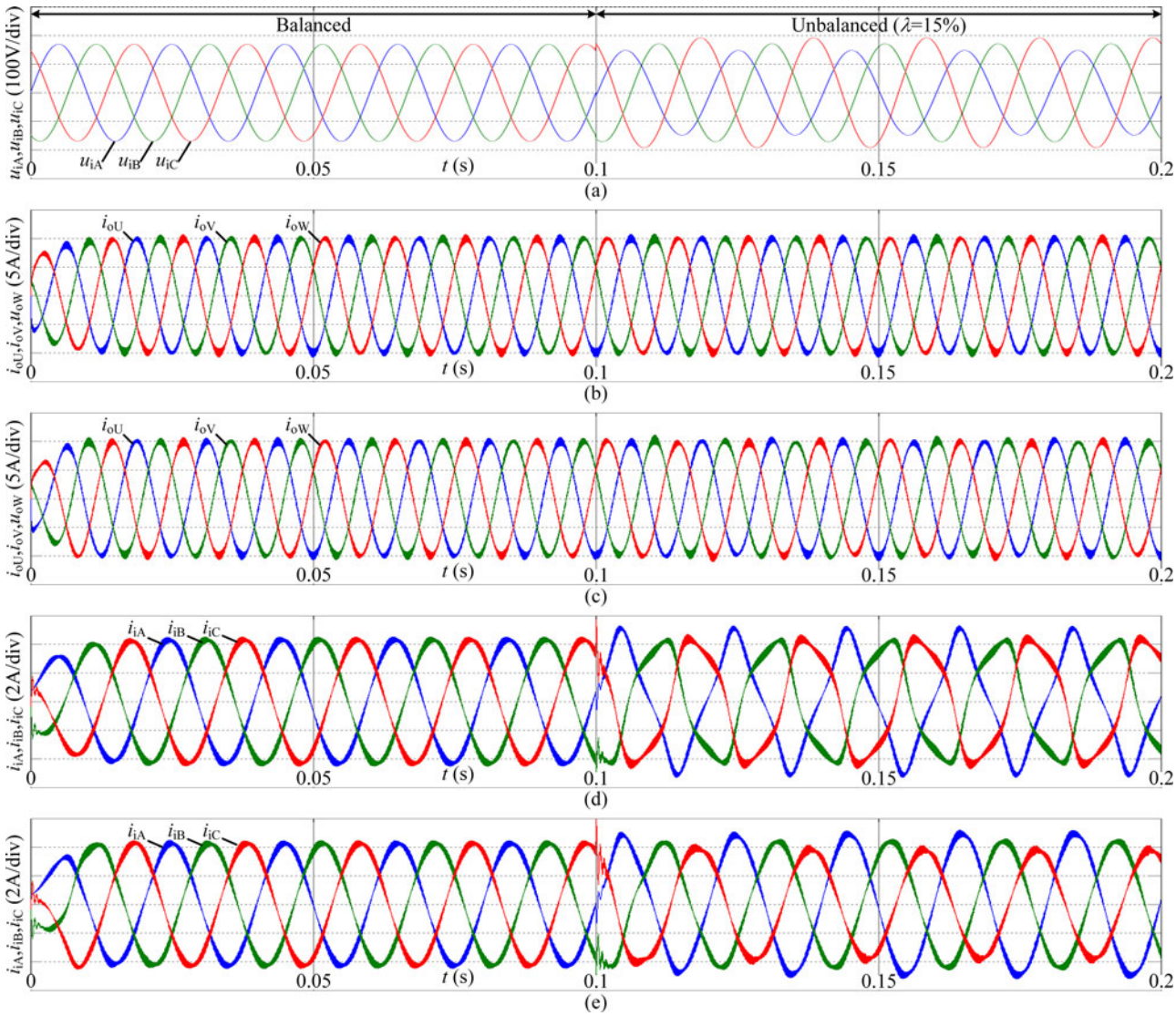

Fig. 9. Simulation results: (a) input voltages, (b) output currents with conventional control method, (c) output currents with the proposed control strategy, (d) input currents with conventional control method, and (e) input currents with the proposed control strategy.

It can be found from (15) and (16) that the gain of $H_P(s)$ at $2\omega_i$ is zero due to the infinite gain of $F_P(s)$ at $2\omega_i$, regardless of the gain of $G_{\mathrm{IP}}(s)$ at $2\omega_i$. Therefore, the power disturbance ΔP_i of $2\omega_i$ cannot be transferred to the actual input active power. This means that the closed-loop control of input active power can eliminate the power harmonic caused by the closed-loop control of input currents and thus the waveform quality of output currents could be maintained.

D. Effect of Active Power Control on the Input Current Control

In the analysis of input current feedback control in Section III-B, the effect of closed-loop control of input active power is not considered. Namely, the modified active power P_i^{**} generated by the active power control loop is assumed to be constant, just the same with the unmodified value P_i^*. This part proves that the assumption is reasonable.

Since $F_P(s)$ has infinite gain at $2\omega_i$, the additional control signal P_{ie}^* output by it could completely compensate the power disturbance ΔP_i caused by the input current control. Consequently, P_{ie}^* is equal to ΔP_i at the steady state. According to Fig. 8 and (14), the modified active power P_i^{**} at steady state can be written as

$$P_i^{**} = P_i^* - P_{\mathrm{ie}}^* = P_i^* - \lambda P_i^* \cos\left(2\omega_i t + \varphi_{\mathrm{iup}} - \varphi_{\mathrm{iun}}\right). \tag{17}$$

Obviously, P_i^{**} contains an ac component whose frequency is $2\omega_i$. With P_i^* in (3) replaced by P_i^{**} and $\varphi_i = 0$ substituted into (3), the input current reference values $i_{i\alpha}^*$ and $i_{i\beta}^*$ are

$$\begin{cases} i_{i\alpha}^* = \dfrac{P_i^* u_{i\alpha}}{1.5(u_{i\alpha}^2 + u_{i\beta}^2)} - \dfrac{P_{\mathrm{ie}}^* u_{i\alpha}}{1.5(u_{i\alpha}^2 + u_{i\beta}^2)} \\ i_{i\beta}^* = \dfrac{P_i^* u_{i\beta}}{1.5(u_{i\alpha}^2 + u_{i\beta}^2)} - \dfrac{P_{\mathrm{ie}}^* u_{i\beta}}{1.5(u_{i\alpha}^2 + u_{i\beta}^2)}. \end{cases} \tag{18}$$

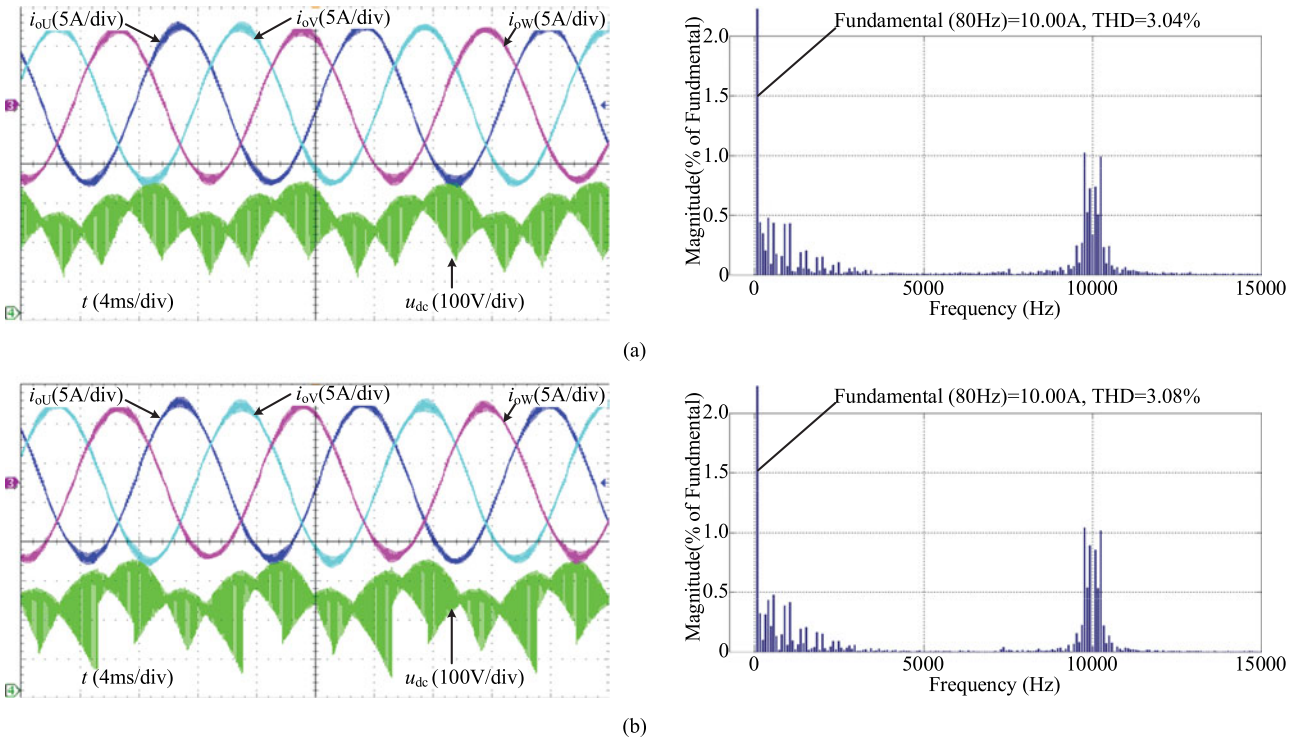

Fig. 10. When the unbalanced degree of input voltages is 15%, waveforms of output currents (i_{ou}, i_{oV}, i_{oW}) and dc-bus voltage (u_{dc}) and the harmonic distribution of phase-U output current: (a) with conventional control method and (b) with the proposed strategy.

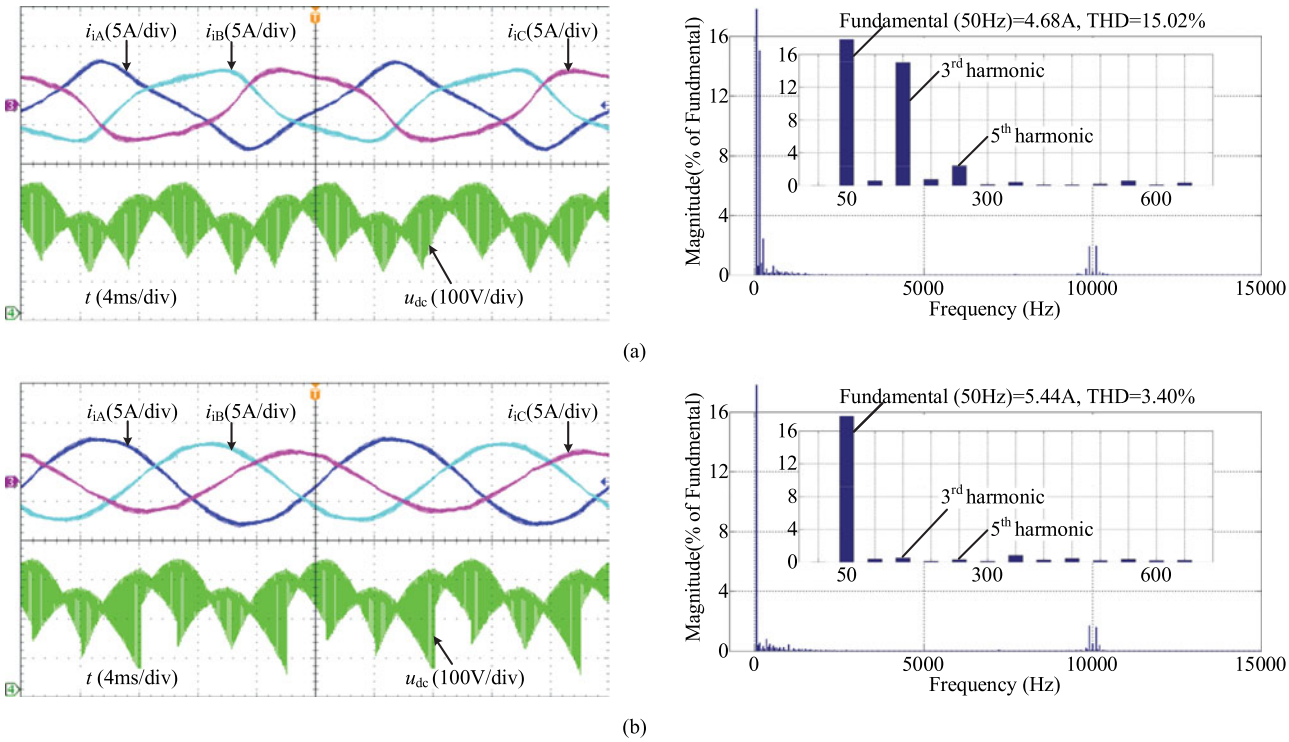

Fig. 11. When the unbalanced degree of input voltages is 15%, waveforms of input currents (i_{iA}, i_{iB}, i_{iC}) and dc-bus voltage (u_{dc}) and the harmonic distribution of phase-A input current: (a) with conventional control method and (b) with the proposed strategy.

According to (3) and (7), the Fourier series of the first items on the right hand of the equations in (18) are composed of the third, fifth, and other odd harmonics in addition to the fundamental components. Considering that the frequency of P_{ie}^{*} is $2\,\omega_i$, it is easy to find that the second term on the right hand of equation (18) also contains third, fifth, and other odd harmonics. Therefore, the input active power feedback control changes the contents of the odd harmonics in the input reference currents $i_{i\alpha}^{*}$ and $i_{i\beta}^{*}$, but does not generate harmonics of new orders. From the viewpoint of input current feedback control, the modified active power reference P_i^{**} with ac component whose frequency is $2\,\omega_i$ has no difference with the unmodified constant value P_i^{*}, since the closed-loop control of input currents can remove the odd harmonics completely.

IV. Simulation and Experimental Verification

A. Simulation and Experimental Conditions

In order to verify the effectiveness of the proposed control strategy, an IMC prototype is built by this paper and a corresponding simulation model is constructed in the MATLAB/Simulink software.

To produce the unbalanced input voltages, a programmable ac power source is selected as the power supply of IMC. In simulation and experiments, the input frequency is 50 Hz, and the phase difference between each two phases is 120°. The amplitude of phase-B input voltage is fixed at 169.7 V (corresponding to RMS 120 V). Different unbalanced degrees are achieved by changing the amplitudes of the other two phases. The amplitudes of three phases input voltages, the positive sequence voltages, and the negative sequence voltages under different unbalanced degrees are shown in Table I.

The parameters of the experimental prototype are shown in Table II. In experiments, the commonly used current feedback control in rotating frame is applied to the output side. The output frequency is 80 Hz and the reference amplitude of the output currents is fixed at 10 A. The SVM of symmetrical switching pattern is applied to IMC, resulting in different switching frequencies of the rectifier stage and inverter stage, which are 10 and 20 kHz separately.

In simulation model, the power switches of IMC are ideal, the control method is realized by Simulink modules, and the rest parameters are the same with those shown in Table II.

In simulation and experimental results, the conventional control method of feedforward compensation with fixed input power factor angle is also comparatively verified, in order to highlight how the proposed control strategy improves the input power quality.

B. Simulation Results

Fig. 9 shows the simulation results. Three-phase input voltages are illustrated in Fig. 9(a). The total simulation time is 0.2 s. The input voltages are balanced in the first 0.1 s while are unbalanced in the last 0.1 s with an unbalanced degree of 15%. Fig. 9(b) and (c) shows the output currents with conventional control method and the proposed strategy, respectively. From these two subfigures, it is found that the output currents with the two methods are all sinusoidal no matter whether the input voltages are balanced or not. Fig. 9(d) and (e) shows the input currents. When input voltages are balanced, the input currents are sinusoidal with both methods. However, in the unbalanced case, the input currents are severely distorted with the conventional control method, but are sinusoidal with the proposed strategy. In summary, the simulation results prove that compared with the conventional control method, the proposed strategy can improve the input currents dramatically while maintain the waveform quality of output currents.

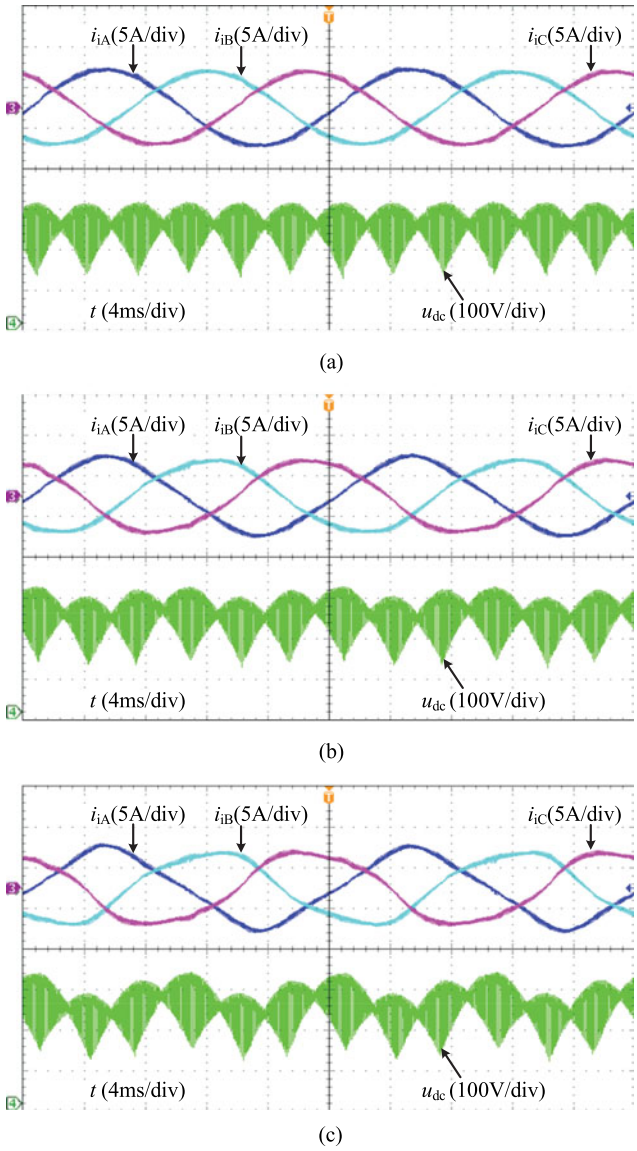

Fig. 12. Waveforms of input currents (i_{iA}, i_{iB}, i_{iC}) and dc-bus voltage (u_{dc}) with the conventional control method under different unbalanced degree λ: (a) $\lambda = 0$ (input voltages are balanced), (b) $\lambda = 5\%$, and (c) $\lambda = 10\%$.

C. Experimental Results

In experiments, the dc-bus voltage, input and output currents are measured with voltage probes and current probes separately

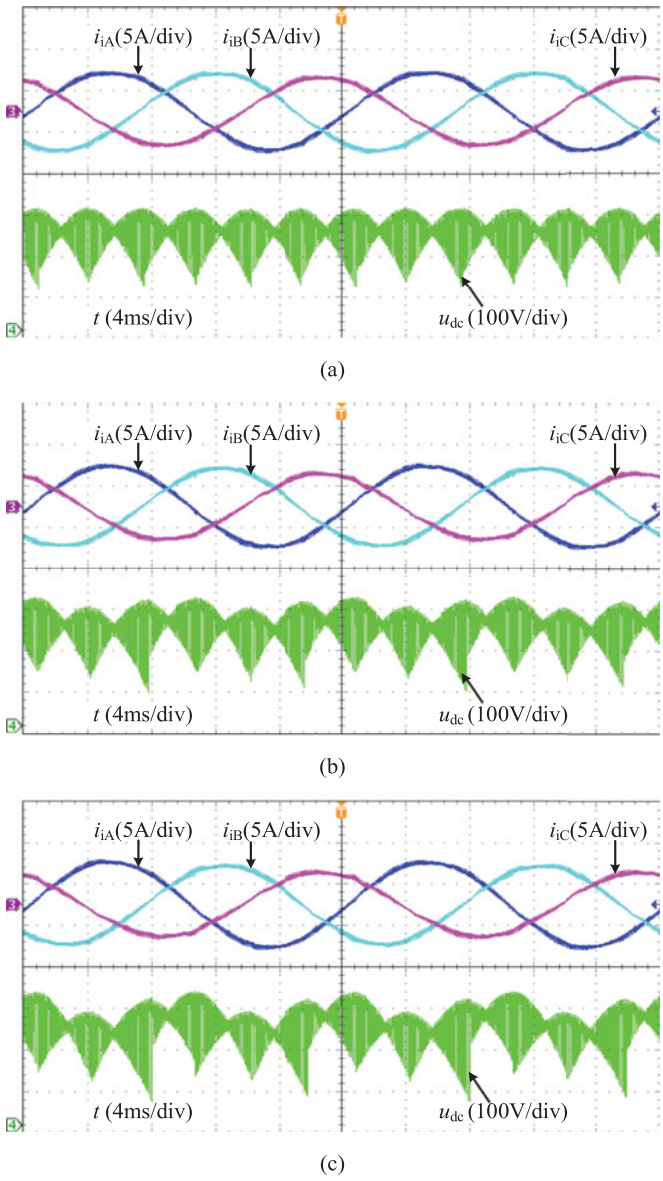

Fig. 13. Waveforms of input currents (i_{iA}, i_{iB}, i_{iC}) and dc-bus voltage (u_{dc}) with the proposed method under different unbalanced degree λ: (a) λ = 0 (input voltages are balanced), (b) λ = 5%, and (c) λ = 10%.

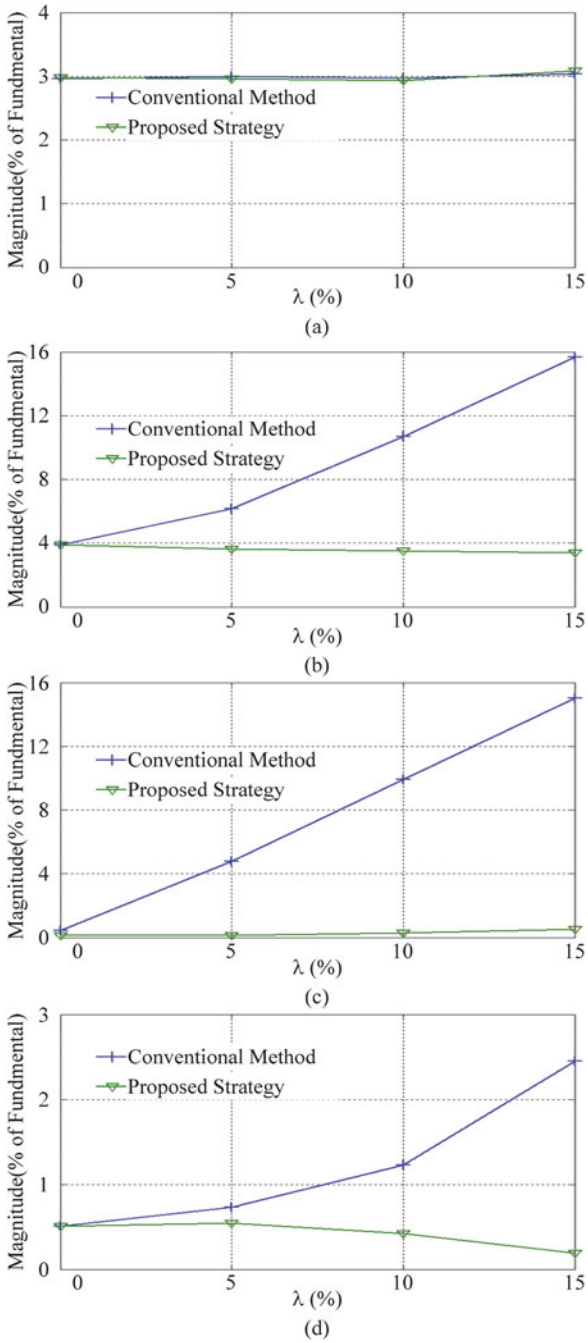

Fig. 14. When the unbalanced degree of input voltages varies in the range [0, 15%], the harmonic contents of phase-U output current and phase-A input current with the conventional control method and the proposed strategy: (a) THD of output current, (b) THD of input current, (c) content of third harmonic in input current, and (d) content of fifth harmonic in input current.

whose bandwidths are 30 MHz. The measured data are also used for harmonic analysis in the MATLAB software.

Fig. 10 shows the three-phase output currents and the harmonic distributions of phase-U output current with the conventional control method and the proposed strategy, when the unbalanced degree of input voltages is 15%. In addition, the waveform of the dc-bus voltage u_{dc} is also given in Fig. 10, so as to indicate that the input voltages are unbalanced. As can be seen from Fig. 10, the contents of low-order harmonics in output currents with the two control methods are less than 0.5%, even if the unbalanced degree of input voltages is up to 15%, showing satisfactory waveform quality. The total harmonic distortion (THD) of output currents is larger than 3.0% due to the high-order harmonics around the switching frequency, which can be reduced by increasing the value of load inductor or switching frequency. Fig. 11 shows the input currents and the harmonic distribution of phase-A input current with the two control methods. With the conventional control method, the THD of input current is up to 15.02%, the content of third harmonic is about 15%, and the content of fifth harmonic is about 2%, which is corresponding to the theoretical analysis in Section III-A. On the contrary, the THD of input current drops to 3.40% by adopting the proposed control strategy. In particular, the contents of the major low-order harmonics are less than 1%, indicating that

sinusoidal input currents are obtained. The high-order harmonics contribute to the THD of input currents, which can be reduced by increasing the damping resistor R_d [26] or by applying active damping control strategy [20], [22], [27].

The conventional control method and the proposed strategy are further comparatively evaluated under different unbalanced degree of input voltages. The waveforms of output currents with both methods are almost the same with those shown in Fig. 10, but the waveforms of input currents are different which are presented in Figs. 12 and 13. By comparing Figs. 12 and 13, it can be found that the input currents with conventional control method become more and more distorted with the increase of unbalanced degree λ. On the contrary, the input currents with the proposed method maintain sinusoidal when λ varies. The harmonic analysis results of output currents and input currents are shown in Fig. 14. It is found from Fig. 14(a) that both the two methods can achieve satisfactory waveform quality of output currents when the unbalanced degree varies from 0% to 15%, since the THDs are all around 3.0%. Fig. 14(b) shows the THDs of input currents with the two control methods. It is clear that the THD of input current with the conventional control method increases rapidly to 15%, but keeps below 4% with the proposed control strategy. According to the analysis in Section III, the third and fifth harmonics are the primary harmonics, and thus they are illustrated in Fig. 14(c) and (d). With the increasing unbalanced degree λ, the contents of the third and fifth harmonics with conventional control method both go up at the rate similar with that shown in Fig. 5, but are suppressed to 1% and lower with the proposed control strategy.

From Figs. 11 to 14, it can be concluded that compared with the conventional control method, the proposed strategy can improve the waveform quality of input currents remarkably when the unbalanced degree of input voltages are in the considered range of [0, 15%]

V. Conclusion

The feedback control strategy on the input side of MC is proposed by this paper based on a control method which enables input reference currents to be modifiable. This control strategy includes closed-loop control of input currents and input active power. By designing appropriate controllers, the input control object can be achieved without degrading the output performance. The proposed control strategy not only addresses the issue that closed-loop control of input currents is difficult to realize, but also helps to increase the degree of freedom and robustness of MC.

This paper then adopts the proposed control strategy to eliminate the input current harmonics under unbalanced input voltages, with resonant controllers designed in the active power loop and input current loop. By applying the proposed control strategy, sinusoidal input currents are obtained, while waveform quality of output currents is maintained. The simulation and experimental results demonstrate that the proposed strategy obtains sinusoidal input currents while maintains good waveform quality of output currents, when the unbalanced degree of input voltages is up to 15%.

References

[1] T. Friedli, J. W. Kolar, J. Rodriguez, and P. W. Wheeler, "Comparative evaluation of three-phase ac-ac matrix converter and voltage dc-link back-to-back converter systems," *IEEE Trans. Ind. Electron.*, vol. 59, no. 12, pp. 4487–4510, Dec. 2012.

[2] L. Empringham, J. Kolar, J. Rodriguez, P. W. Wheeler, and J. C. Clare, "Technological issues and industrial application of matrix converters: A review," *IEEE Trans. Ind. Electron.*, vol. 60, no. 10, pp. 4260–4271, Oct. 2013.

[3] S. S. Sebtahmadi, H. Pirasteh, S. H. A. Kaboli, A. Radan, and S. Mekhilef, "A 12-sector space vector switching scheme for performance improvement of matrix-converter-based DTC of IM drive," *IEEE Trans. Power Electron.*, vol. 30, no. 7, pp. 3804–3817, Jul. 2015.

[4] J. Monteiro, J. F. Silva, S. F. Pinto, and J. Palma, "Linear and sliding-mode control design for matrix converter-based unified power flow controllers," *IEEE Trans. Power Electron.*, vol. 29, no. 7, pp. 3357–3367, Jul. 2014.

[5] X. Liu, P. C. Loh, P. Wang, F. Blaabjerg, Y. Tang, and E. A. Al-Ammar, "Distributed generation using indirect matrix converter in reverse power mode," *IEEE Trans. Power Electron.*, vol. 28, no. 3, pp. 1072–1082, Mar. 2013.

[6] J. Kolar, T. Friedli, J. Rodriguez, and P. W. Wheeler, "Review of three phase PWM ac-ac converter topologies," *IEEE Trans. Ind. Electron.*, vol. 58, no. 11, pp. 4988–5006, Nov. 2011.

[7] J. Haruna and J. Itoh, "Behavior of a matrix converter with a feed back control in an input side," in *Proc. Int. Power Electron. Conf.*, 2010, pp. 1202–1207.

[8] J. Haruna, J. Itoh, "Control strategy for a matrix converter with a generator and a motor," in *Proc. 26th IEEE Appl. Power Electron. Conf. Expo.*, 2011, pp. 1782–1789.

[9] V. Kumar and R. R. Joshi, "DSP-based matrix converter operation under various abnormal conditions with practicality," in *Proc. IEEE Int. Conf. Power Electron. Drives Energy Syst.*, Jan. 8–11, 1996, vol. 2, pp. 1–4.

[10] P. Nielsen, F. Blaabjerg, and J. K. Pedersen, "Space vector modulated matrix converter with minimized number of switchings and a feedforward compensation of input voltage unbalance," in *Proc. IEEE Int. Conf. Power Electron. Drives Energy Syst.*, Jan. 8–11, 1996, vol. 2, pp. 833–839.

[11] D. Casadei, G. Serra, and A. Tani, "Reduction of the input current harmonic content in matrix converters under input/output unbalance," *IEEE Trans. Ind. Electron.*, vol. 45, no. 3, pp. 401–411, Jun. 1998.

[12] X. Wang, H. Lin, H. She, and B. Feng, "A research on space vector modulation strategy for matrix converter under abnormal input-voltage conditions," *IEEE Trans. Ind. Electron.*, vol. 59, no. 1, pp. 93–104, Jan. 2012.

[13] F. Blaabjerg, D. Casadei, C. Klumpner, and M. Matteini, "Comparison of two current modulation strategies for matrix converters under unbalanced input voltage conditions," *IEEE Trans. Ind. Electron.*, vol. 49, no. 2, pp. 289–296, Apr. 2002.

[14] J. K. Kang, H. Hara, A. M. Hava, E. Yamamoto, E. Watanabe, and T. J. Kume, "The matrix converter drive performance under abnormal input voltage conditions," *IEEE Trans. Power Electron.*, vol. 17, no. 5, pp. 721–730, Sep. 2002.

[15] Y. Yan, H. An, T. Shi, and C. Xia, "Improved double line voltage synthesis of matrix converter for input current enhancement under unbalanced power supply," *IET Power Electron.*, vol. 6, no. 4, pp. 798–808, Apr. 2013.

[16] J. D. Dasika and M. Saeedifard, "An online modulation strategy to control the matrix converter under unbalanced input conditions," *IEEE Trans. Power Electron.*, vol. 30, no. 8, pp. 4423–4436, Aug. 2015.

[17] X. Li, M. Su, Y. Sun, H. Dan, and W. Xiong, "Modulation strategies based on mathematical construction method for matrix converter under unbalanced input voltages," *IET Power Electron.*, vol. 6, no. 3, pp. 434–445, Mar. 2013.

[18] J. Lei, B. Zhou, J. Bian, X. Qin, and J. Wei, "A simple method for sinusoidal input currents of matrix converter under unbalanced input voltages," *IEEE Trans. Power Electron.*, vol. 31, no. 1, pp. 21–25, Jan. 2016.

[19] S. Li, X. Wang, Z. Yao, T. Li, and Z. Peng, "Circulating current suppressing strategy for MMC-HVDC based on nonideal proportional resonant controllers under unbalanced grid conditions," *IEEE Trans. Power Electron.*, vol. 30, no. 1, pp. 387–397, Jan. 2015.

[20] J. Lei, B. Zhou, X. Qin, J. Wei, and J. Bian, "Active damping control strategy of matrix converter via modifying input reference currents," *IEEE Trans. Power Electron.*, vol. 30, no. 9, pp. 5260–5271, Sep. 2015.

[21] J. Rodriguez, M. Rivera, J. W. Kolar, and P. W. Wheeler, "A review of control and modulation methods for matrix converters," *IEEE Trans. Ind. Electron.*, vol. 59, no. 1, pp. 58–70, Jan. 2012.

[22] Y. Sun, M. Su, X. Li, H. Wang, and W. Gui, "A general constructive approach to matrix converter stabilization," *IEEE Trans. Power Electron.*, vol. 28, no. 1, pp. 418–431, Jan. 2013.
[23] H. Akagi, Y. Kanazawa, and A. Nabae, "Generalized theory of the instantaneous reactive power in three-phase circuits," in *Proc. Int. Power Electron. Conf.*, 1983, pp. 1375–1386.
[24] *IEEE Recommended Practice for Monitoring Electric Power Quality*, IEEE Std. 1159-2009 (Revision of IEEE Std. 1159–1995, pp. c1–c81, June 2009.
[25] D. N. Zmood and D. G. Holmes, "Stationary frame current regulation of PWM inverters with zero steady-state error," *IEEE Trans. Power Electron.*, vol. 18, no. 3, pp. 814–822, May 2003.
[26] J. Andreu, I. Kortabarria, E. Ormaetxea, E. Ibarra, J. L. Martin, and S. Apinaniz, "A step forward towards the development of reliable matrix converters," *IEEE Trans. Ind. Electron.*, vol. 59, no. 1, pp. 167–183, Jan. 2012.
[27] J. Lei, B. Zhou, X. Qin, J. Bian, and J. Wei, "Stability improvement of matrix converter by digitally filtering the input voltages in stationary frame," *IET Power Electron.*, Nov. 2015, DOI:10.1049/iet-pel.2015.0163.

Jiaxing Lei (S'14) was born in Dazhou, China, 1991. He received the B.S. degree from the Nanjing University of Aeronautics and Astronautics, Nanjing, China, in 2012, where he has been working toward the Ph.D. degree since 2012.

His main research interests are in matrix converters and its applications in aerospace power system.

Bo Zhou was born in Wenzhou, Zhejiang Province, China, in 1961. He received the B.S. degree from Zhejiang University, Hangzhou, China, in 1983, and the M.S. degree from Chongqing University, Chongqing, China, in 1986. Then, he was with the Nanjing University of Aeronautics and Astronautics (NUAA), Nanjing, China, where he received the Ph.D. degree in 2000.

He is currently a Professor in the College of Automation Engineering, NUAA, and is the Director of the Jiangsu Key Laboratory of New Energy Generation and Power Conversion. His research interests include power converter, electrical machine driving systems, and renewable power systems.

Dr. Zhou received the State Technological Invention Second-Class Award in 2009, the Geneva International Invention Gold Award in 2011, and the Defense Technological Invention first prize in 2008.

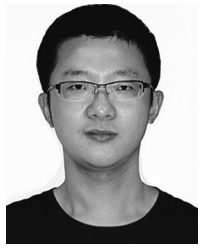

Jinliang Bian was born in Nantong, China, 1990. He received the B.S. degree from the Nanjing University of Aeronautics and Astronautics, Nanjing, China, in 2013, where he has been working toward the M.S. degree since 2013.

His main research interests are in matrix converters and its applications in aerospace power system.

Jiadan Wei (M'10) was born in Danyang, Jiangsu Province, China, in 1981. He received the B.S. and Ph.D. degrees in electrical engineering from the Nanjing University of Aeronautics and Astronautics (NUAA), Nanjing, China, in 2003 and 2009, respectively.

He is currently an Associate Professor in the College of Automation Engineering, NUAA. His research interests are in the power electronics, motion control system, and renewable power systems.

Yiqi Zhu was born in Haining, China, in 1993. She is now an undergraduate student in the Nanjing University of Aeronautics and Astronautics, Nanjing, China, where she has been working toward the B.S. degree since 2016.

Her research interests include matrix converter and its control strategy.

Jiang Yu was born in Zi Gui, China, in 1978. He received the Master's degree from the Xi'an University of Technology, Xi'an, China, in 2012.

He has been a Senior Engineer, as researching in power electronic technology and its application in aerospace power system.

Yang Yang was born in Wei Nan, China, in 1988. She received the Master's degree from North Western Polytechnical University, Xi'an, China, in 2014.

Her main research interests are in simulation technology and its application in aerospace power system.